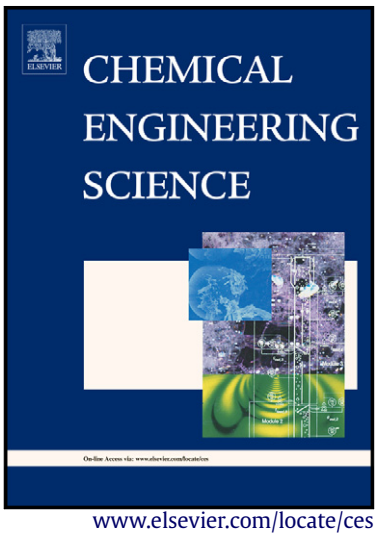

www.elsevier.com/locate/ces

Adsorption of CH_4 and CH_4/CO_2 Mixtures in Carbon Nanotubes and Disordered Carbons: A Molecular Simulation Study

Lang Liu, David Nicholson, Suresh K. Bhatia

PII: S0009-2509(14)00386-8
DOI: http://dx.doi.org/10.1016/j.ces.2014.07.041
Reference: CES11774

To appear in: *Chemical Engineering Science*

Received date: 30 April 2014
Revised date: 14 July 2014
Accepted date: 20 July 2014

Cite this article as: Lang Liu, David Nicholson, Suresh K. Bhatia, Adsorption of CH_4 and CH_4/CO_2 Mixtures in Carbon Nanotubes and Disordered Carbons: A Molecular Simulation Study, *Chemical Engineering Science,* http://dx.doi.org/10.1016/j.ces.2014.07.041

Adsorption of CH_4 and CH_4/CO_2 Mixtures in Carbon Nanotubes and Disordered Carbons: A Molecular Simulation Study

Lang Liu, David Nicholson, Suresh K. Bhatia*

School of Chemical Engineering

The University of Queensland

Brisbane, QLD 4072, Australia

We report a comparison of the adsorption of CH_4 and CO_2/CH_4 mixtures of different composition in three different types of nanoporous carbons including carbon nanotubes, and activated carbon fiber (ACF-15) and silicon carbide derived carbon (SiC-DC) having distinctly different disordered structures, using Monte Carlo simulation. CO_2 is represented as a linear molecule, and both the united-atom and full-atom models are investigated for CH_4. It is found that the united-atom model of CH_4 overestimates the adsorption capacity of CH_4 in all these adsorbents compared to the 5-site model, as a consequence of the enhanced 1-site CH_4-adsorbent potential energy. Moreover, the selectivities of the nanoporous carbons for CO_2 relative to CH_4 calculated using the 1-site CH_4 model are underestimated compared to those from the 5-site model, at pressures up to 3.0 MPa. However, differences in the structural disorder of porous carbon models have little impact on CO_2 selectivity. Our simulations reveal that the selectivity of an adsorbent for a particular species is strongly dependant on adsorbate-adsorbate interaction effects, comprising the adsorbate-adsorbate potential interactions and an adsorbate sieving effect. As a balance between the confinement and adsorbate-adsorbate effects, it is found that increasing the concentration of CO_2 in the gas phase increases the selectivity of (10, 10) CNT dramatically, while having negligible impact on the selectivities in amorphous carbons. Further, it is shown that increasing the temperature reduces the performance of all the carbons in separating CO_2, and that an isolated (7, 7) CNT has the best performance for CO_2/CH_4 separation in comparison to the disordered nanoporous carbons investigated.

Keywords: Carbon dioxide; methane; Carbon nanotubes; porous carbons; Carbon dioxide-methane separation; simulation

---

*To whom correspondence may be addressed. Email: s.bhatia@uq.edu.au.

1 Introduction

Natural gas has been regarded as an ideal substitute for fossil fuels because of low emissions of greenhouse gases and particulate matter after combustion (Martín-Calvo *et al*., 2008). CO_2 is one of the major contaminants that must be removed from natural gas, since it reduces its energy content and corrodes pipelines in the presence of water. Consequently, a variety of approaches have been proposed to separate CO_2 from natural gas, including chemical conversion, solvent absorption, membrane separation, and adsorptive separation. Among these, adsorptive separation has shown to be technically and economically favourable (Babarao *et al*., 2009). Porous carbons have long been studied as promising adsorbent materials for CO_2 capture (Lu *et al*., 2008; Pevida *et al*., 2008; Przepiórski *et al*., 2004) and separation from gas mixtures (Ducrot-Boisgontier *et al*., 2010; Heuchel *et al*., 1999), due to their high surface area, finely-tuneable pore size distribution and economical production (Presser *et al*., 2011). It has been shown that suitable tailoring of the pore structure in porous carbons by controlling the synthesis process can improve the efficiency of separating CO_2 from CO_2/CH_4 mixtures (Dash *et al*., 2006; Gogotsi *et al*., 2003; Nicholson and Gubbins, 1996; Cracknell *et al*., 1996). However, not only the pore size distribution, but also the morphology of porous carbons can vary significantly depending on the synthesis procedure, and can range from extremely disordered materials, such as Silicon Carbide Derived Carbon (SiC-DC) (Farmahini *et al*., 2013; Nguyen *et al*., 2009), activated carbon fibre ACF15 (Nguyen *et al*., 2008) to materials that are intrinsically well defined such as carbon nanotubes (CNTs) (Presser *et al*., 2011). Consequently, understanding the effect of morphology on the adsorption of CH_4 and CO_2/CH_4 mixtures in porous carbons is essential for optimizing adsorbent structure for both CH_4 storage and for CO_2/CH_4 separation. Moreover, since CNTs have been shown to possess superior transport properties for CH_4 and CO_2 (Skoulidas *et al*., 2002; Skoulidas *et al*., 2006), it is important to know the adsorption selectivity of CNTs for CO_2 over CH_4 in comparison to that of porous carbons having realistic structures.

As there are always technical challenges in performing experimental measurements of multicomponent adsorption in porous carbons, molecular simulation methods provide an efficient and rigorous alternative to investigate the multicomponent adsorption in all kinds of porous carbons by explicitly considering the intermolecular and pore-wall interactions. The choice of molecular models plays an essential role in predicting adsorption behaviour. Do and Do (2005) found the adsorption of CH_4 in graphitic slit pores at both sub- and super-critical temperatures was over predicted by the 1-site model compared to the full-atom model; this

was ascribed by these authors to the more efficient packing of the 1-site CH_4. Similarly, Bhatia and Nicholson (2012) also observed that adsorption of 1-site CH_4 was overestimated compared to 5-site CH_4 in their study of the adsorption of CH_4 in silica nanopores. However, these authors attributed this overestimation to the enhanced adsorbate-adsorbent potential energy for the 1-site CH_4. Cracknell *et al*. (1993, 1994) studied the adsorption of ethane and methane from equimolecular mixtures in graphitic slit pores and found that the molecular model strongly influenced the calculated adsorption selectivity for ethane, which increased dramatically when ethane was modelled as two sites rather than a single site molecule. Moreover, increasing the bond length to create a pseudo-ethane reduced the selectivity significantly because of the increased hindrance to rotation in the confined space of the micropores. Despite these observations, in most simulations and theoretical investigations of CO_2/CH_4 adsorption (Babarao *et al*., 2006; Babarao and Jiang, 2009; Bhatia *et al*., 2004; Heuchel *et al*., 1999; Liu and Smit, 2009; Palmer *et al*., 2011; Yang and Zhong, 2006), CH_4 is represented as a united atom and CO_2 is represented as a 3-site linear molecule. Little is known about the effect of the molecular model of CH_4 on the adsorption of CH_4 and CO_2/CH_4 mixtures in CNTs and realistic porous carbons, which will be investigated in this work.

An important feature of the co-adsorption of mixture in confined space is that the selectivity is a result of the interplay of adsorbate-adsorbent and adsorbate-adsorbate interactions. Babarao *et al*. (2009) compared the equimolar adsorption of CO_2/CH_4 mixture in a series of metal-organic frameworks (MOFs) and found that, except for IRMOF-13, the selectivities of all other MOFs for CO_2 over CH_4 increased monotonically with pressure, as the cooperative attractions between adsorbed CO_2 molecules promoted further adsorption of CO_2. The initial decrease of the selectivity in IRMOF-13 is interpreted as a consequence of the reduced adsorbate-adsorbent interactions, since CO_2 molecules tend to occupy larger pores with increasing pressure. Kurniawan *et al*. (2006) examined the effect of composition on CO_2/CH_4 separation at 318 K in graphitic slit pores of width 1.5 nm. It was shown that at a pressure of 10 bar the selectivity increases significantly with increasing CO_2 concentration in the bulk phase. Similarly, based on their experimental studies Heuchel *et al*. (1999) reported that increasing the fraction of CO_2 in the bulk phase from 0.21 to 0.92 significantly increases the selectivity of activated carbon A35/4 for CO_2 over CH_4, at pressures up to 15 bar. Martín-Calvo *et al*. (2008) found similar, but smaller, effects of composition on CO_2/CH_4 separation in Cu-BTC. Thus, it is clear that effects related to adsorbate-adsorbate interactions play a

crucial role in determining the selectivity for a particular species. In most simulation studies these effects are interpreted as the balance between the energetic and entropic effects (Babarao *et al*., 2006; Babarao and Jiang, 2009; Babarao *et al*., 2009; Herm *et al*., 2011; Liu and Smit, 2009, 2010; Palmer *et al*., 2011). In terms of CO_2/CH_4 adsorption, increasing the loading would increase the CO_2-adsorbates (CO_2+CH_4) pair interactions more significantly than the counterparts for CH_4-adsorbates (Babarao *et al*., 2009). This would subsequently promote the adsorption of CO_2 over CH_4. On the other hand, the entropic effect is simply interpreted as the packing-related restrictions imposed by the pore walls or by neighbouring molecules on the orientational freedom of adsorbates, which may be expected to supress the adsorption of linear CO_2 (Nicholson and Gubbins, 1996). Additionally, the more strongly adsorbed species will tend to apply a sieving effect on the components, enhancing the selectivity. Consequently, in this investigation, the effect of composition in CNTs and porous carbons is analysed with regard to the adsorbate sieving effect.

We report here a grand canonical Monte Carlo (GCMC) simulation study of the adsorption of CH_4 and CO_2/CH_4 mixtures in a variety of armchair CNTs, ACF-15 and SiC-DC, to investigate the effects of the morphology of porous carbons and of the molecular model of CH_4 on the adsorption of CH_4 and CO_2/CH_4 mixture in porous carbons. Three compositions of CO_2/CH_4 mixtures, having CO_2 concentrations of 5%, 25% and 50% on a molar basis, are considered at 300 K to examine the effect of composition on separating CO_2 from natural gas using CNTs and realistic porous carbons. In addition, the effect of temperature on the adsorption of CO_2/CH_4 is examined, and the optimal diameter of CNTs for CO_2 separation from natural gas is determined in this investigation. The study comprises a wide-ranging survey of the possibilities for CO_2 separation from natural gas using carbon based adsorbents.

2 Simulation details

2.1 Carbon Models

Carbon nanotubes are modelled as a graphite sheet wrapped into cylindrical shape, providing ordered cylindrical pores for adsorption. As indicated above, two types of disordered nanoporous carbons, ACF-15 and SiC-DC, having distinctly different structures, are also investigated to reveal the potential of the CNTs in separating CO_2 from natural gas. The atomistic configurations of the CNT, ACF-15 and SiC-DC are illustrated in Figure 1, and were treated as rigid structures with a Lennard-Jones (L-J) particle on each site. In the present work, the pore volume of each CNT studied is predetermined, since we exclusively consider

the adsorption of CH_4 and CO_2/CH_4 mixtures in the internal space of isolated CNTs. However, for the disordered carbons, ACF-15 and Si-CDC, their geometric pore size distributions are determined using the method proposed by Gelb and Gubbins (1999), and depicted in Figure 1(d). The atomistic structures for both disordered carbons were previously modelled in our laboratory using hybrid reverse Monte Carlo (HRMC) simulations (Farmahini *et al*., 2013; Nguyen *et al*., 2009). For the ACF-15, the experimental material was an ACC-5092-15 activated carbon fiber, provided by Kynol Corporation. The SiC-DC was synthesised in our laboratory by oxidation of a βSiC precursor in a pure chlorine atmosphere at 1073K. The disordered nature of the ACF-15 and SiC-DC was confirmed by the results from X-ray diffraction and high-resolution transmission electron microscopy (HRTEM) characterization. The reconstructed atomistic structures for ACF-15 and SiC-DC have been validated by comparing the adsorption of Ar, CO_2, and CH_4 against experimental data over a wide range of temperature and pressure (Farmahini *et al*., 2013; Nguyen *et al*., 2009; Nguyen *et al*., 2008).

The armchair CNTs had diameters ranging from 0.81 to 2.03 nm. The ACF-15 was modelled as a periodic porous material with dimension of its unit cell obtained as $2.95\times2.98\times3.02\,\text{nm}^3$. 1166 carbon atoms were placed in the unit cell, resulting in the bulk carbon density, $\rho_{bc}=0.88$ g/cm^3. In addition, the unit cell of SiC-DC was obtained as $4.0\times4.0\times4.0$ nm^3, containing 3052 carbon atoms. The bulk carbon density for SiC-DC is 0.95 g/cm^3. As illustrated in Figure 1, the structure of the porous carbons ranges from highly ordered to completely disordered.

2.2 Molecular models

The 3-site (EPM2) linear model proposed by Harris and Yung (1995), which accounts for the quadrupole of CO_2 explicitly by assigning a point-charge on each atom, was chosen to represent CO_2. The model has been shown to represent the packing configuration of CO_2 molecules in narrow carbon slits accurately (Bhatia *et al*., 2004). Both the spherical model (Hirschfelder *et al*., 1954) and the full-atom model proposed by Kollman and co-workers (Sun *et al*., 1992) for CH_4 were investigated. In the spherical model, CH_4 is treated as a single L-J particle. In the 5-site model, all the atoms are explicitly included as L-J particles, each carrying a partial charge. The potential energy parameters and the atomistic configurational parameters of CO_2, 1-site and 5-site CH_4 are given in Table 1. We adopted the Steele (1978)

parameters to represent the C atoms in the adsorbents, with $\sigma_C = 0.34\,\text{nm}$, $\varepsilon_C / k_B = 28K$. The potential energies of the adsorbate-adsorbate and adsorbate-adsorbent are described by the dispersion-repulsion and electrostatic interactions between sites *i* and *j*, following

$$u_{ij}^{(\alpha,\beta)} = 4\varepsilon_{ij}^{(\alpha,\beta)}\left[\left(\frac{\sigma_{ij}^{(\alpha,\beta)}}{r_{ij}^{(\alpha,\beta)}}\right)^{12} - \left(\frac{\sigma_{ij}^{(\alpha,\beta)}}{r_{ij}^{(\alpha,\beta)}}\right)^{6}\right] + \frac{1}{4\pi\varepsilon_0}\frac{q_i^{\alpha} q_j^{\beta}}{r_{ij}^{(\alpha,\beta)}} \qquad (1)$$

where $r_{ij}^{(\alpha,\beta)}$ is the distance between two sites *i* and *j* of molecules α and β. The L-J size parameter $\sigma_{ij}^{(\alpha,\beta)}$ and well depth parameter $\varepsilon_{ij}^{(\alpha,\beta)}$ for the unlike interactions were estimated using the Lorentz-Berthelot mixing rules (Allen and Tildesley, 1989). In eqn.(1), the first term on the right hand side represents the dispersive-repulsive component and the second term corresponds to the electrostatic interactions. In the second term, q_i^{α} and q_j^{β} are the partial charges on sites *i* and *j* of molecules α and β, and ε_0 is the permittivity of free space ($\varepsilon_0 = 8.8543\times10^{-12}\ C^2/J\cdot m$). As confirmed in our previous simulations, the adsorption of multisite CO_2 and CH_4 in ACF-15 and SiC-CDC agreed well with the experimental data without any long-range corrections for the coulombic interactions (Farmahini *et al*., 2013; Nguyen *et al*., 2008) because the neutrality of CO_2 and CH_4 and the short-range of the quadrupole moments, leads to the rapid convergence of the electrostatic interactions with molecule-molecule distance. In ACF-15 and SiC-DC, the L-J and coulombic interactions were therefore calculated using center-of-mass cutoff radii of 1.47 and 1.95 nm respectively. However, in the absence of prior results that we could compare with to exclude the effect of long range corrections in CNTs, the Dot Line Method (Tang and Chan, 2004; Zhang *et al*., 2009), which has been proved to be effective for representing the periodic charges of ions in cylindrical pores, was used in present work to capture the adsorbate-adsorbate coulombic interactions in CNTs. Accordingly, the periodic boundary condition is applied only in the axial direction of the CNT, and only the adsorbate-adsorbate and adsorbate-adsorbent interactions within the CNT are considered, while external adsorption is excluded.

2.3 Grand canonical Monte Carlo simulations

GCMC simulations were used to study the adsorption of CH_4 and CO_2/CH_4 mixture in the three different carbon materials at 300 K, 325 K and 350 K, at pressure up to 3.0 MPa. In GCMC simulations, the adsorbate chemical potential μ_a and the system volume *V* and

temperature T are held constant, while the number of adsorbate molecules as well as the location and the orientation of each adsorbed molecule are allowed to fluctuate. Trial moves, included insertion, deletion and displacement of particles, and the numbers of insertion and deletion attempts were set equal to maintain microscopic reversibility. The fugacities corresponding to the selected compositions were determined from the natural gas equation of state (EOS) given by Kunz and Wagner (2012). Each simulation point was averaged over a total of 1.0×10^{8} configurations, after rejecting the first 3×10^{7} to equilibrate the system.

3 Results and Analysis

3.1 Effect of molecular model on the adsorption of CH_4

We first studied the adsorption of pure CH_4 in a (10, 10) CNT, ACF15 and Si-CDC using both the spherical and full-atom models at 300 K to explore the reasons for the enhanced adsorption of spherical CH_4. It is noted that that the bulk densities of CH_4 obtained from the 1-site and 5-site models are quantitatively similar at 300 K, for pressures up to 3.0 MPa, as demonstrated in Figure 2, confirming that the two models are equivalent in the bulk phase.

As illustrated in Figure 3, the adsorbed amount of 1-site CH_4 is higher in all the cases than that of the 5-site CH_4, which accords with the earlier results of Do and Do (2005) and Bhatia and Nicholson (2012). In addition, at high pressures, the deviation between the adsorption of 1-site and 5-site CH_4 in the (10, 10) CNT diminishes with increasing pressure, as the adsorption of CH_4 approaches saturation. However, in ACF-15 and SiC-DC, which have larger adsorption capacities, the adsorption of CH_4 continues to increase with pressure, and the deviation between the adsorbed amounts of 1-site and 5-site CH_4 is maintained over the pressure range investigated.

To determine whether packing or potential energy causes this enhanced adsorption, we investigated the variation in the CH_4-adsorbent and CH_4-CH_4 interaction energies with CH_4 loading. Figure 4, shows the ensemble average values of these interaction energies, computed from the simulations by evaluating the decrement in the potential energy of the system on the successful insertion of an adsorbate molecule. In the (10, 10) CNT, at loadings lower than 2.3 mol/kg, the CH_4-CH_4 interaction energies are almost identical for both models which implies that the packing does not have any significant impact on the adsorption at low loading. As the loading is increased further, the packing effect becomes more important for both models, which is evident from the increase in CH_4-CH_4 interaction energies, indicating that the

intermolecular repulsive interactions are beginning to dominate and the 1-site CH_4 experiences a stronger intermolecular repulsive interaction than the 5-site CH_4. The radial distribution functions for the two models at a loading of 3.75 mol/kg are shown in Figure 5(a) where it is seen that the 5-site CH_4 molecules can pack more closely due to their tetrahedron structure but have a weaker repulsive interaction. This reveals that the packing configuration of 1-site CH_4 is less favorable in the high loading regime, which is associated with the enhanced adsorption of 1-site CH_4. So, the enhanced adsorption of 1-site CH_4 that is observed in the (10, 10) CNT cannot be explained by the packing effect within the pressure range studied. On the other hand, the 1-site CH_4-CNT interaction is much stronger than the counterpart of 5-site CH_4-CNT. We also plotted the center-of-mass density distributions of the 1-site and 5-site CH_4 in the (10, 10) CNT at a loading of 3.75 mol/kg in Figure 5 (b). It is shown that the density distributions for both models are nearly identical and the near coincidence of the density peaks confirms that the effective diameters of these two models are very similar despite the variable orientation of the 5-site model (Bhatia and Nicholson, 2012). It can be concluded that the enhanced adsorption of 1-site CH_4 in CNTs is caused by the lower CH_4-adsorbent energy. However, in disordered ACF15 and SiC-DC with less confinement, the 1-site CH_4-CH_4 energy is marginally stronger than the 5-site CH_4-CH_4 energy. In these adsorbents, the orientations of the 5-site CH_4 molecules at low pressure are more randomly distributed in spaces where there is lower confinement. The slightly enhanced CH_4-CH_4 interaction cannot be responsible for the considerably enhanced 1-site CH_4 adsorption, since it is negligible compared to the CH_4-adsorbent interaction. These results demonstrate that the enhanced adsorption of 1-site CH_4 in ordered and disordered porous carbons can be attributed to the enhanced CH_4-adsorbent energy.

Due to the similarities of the bulk carbon density and pore size distribution for ACF-15 and SiC-DC (Farmahini *et al*., 2013; Nguyen *et al*., 2008), the simulated adsorption isotherms of CH_4 in ACF-15 and SiC-DC are found to be quantitatively similar, both for the 1-site and 5-site CH_4, as shown in Figure 3. It is also observed that for pressures below 0.7 MPa, the adsorption of CH_4 in the (10, 10) CNT having diameter of 1.36 nm is comparable to that in the ACF-15 and SiC-DC, whose pore sizes range from 0.3 nm to 1.1 nm and 0.2 nm to 1.3 nm, respectively (Farmahini *et al*., 2013; Nguyen *et al*., 2008). Note that, both sides of the pore walls are available for the adsorption of CH_4 in ACF-15 and SiC-DC. On the other hand our simulations only consider adsorption in the internal space for CNTs. Consequently, the comparable adsorption of CH_4 in (10, 10) CNT at low pressure is attributed to the enhanced

fluid-solid interaction energy in the nanotube, which is evident from Figure 4(a). It is seen that CH_4-adsorbent interaction energies are quite similar in ACF-15 and SiC-DC, indicating similarity in the degree of confinement in these two structures, and these are much weaker than that in the (10, 10) CNT. The stronger interaction with the CNT is due to its high carbon density (2.25 g/cm^3) and strong confinement resulting from the high curvature of the carbon wall. In summary, our simulations show that the level of disorder of the carbon structure does not significantly affect the adsorption of CH_4 in porous carbons when the pore size distributions as well as the densities of the carbon structures are similar. For the same pore size, the adsorption of CH_4 will be enhanced in the pores formed by curved walls in comparison to the slit pores, due to the overlap of the potential field exerted by the curved walls, and the symmetric molecular structure of methane. Nevertheless, CH_4 adsorbs onto the both sides of the carbon layers in the disordered carbons. As we increase the curvature of a carbon wall, the adsorption of CH_4 will increase on the concave side, but the adsorption on the convex side is too complex to be predicted, which is dependent on the size of the pore located on the convex side and the curvature of the adjacent wall (Palmer *et al*., 2011). Consequently, the effect of curvature on the adsorption of CH_4 in disordered carbons remains an open question, and will be further studied in our future work.

3.2 Effect of the molecular model of CH_4 on CO_2/CH_4 mixture adsorption

Typically, the concentration of CH_4 in natural gas is around 95% (Martín-Calvo *et al*., 2008), consequently we investigated the adsorption of CO_2/CH_4 mixture in (10, 10) CNT, ACF-15 and SiC-DC using the linear CO_2 and 1-site and 5-site CH_4, with 5% CO_2 in the bulk phase. The mixture isotherms at 300 K for the three adsorbents studied are shown in Figure 6. It was found the adsorption of CH_4 is dominant in all the cases, primarily because of its high concentration in the bulk phase. In addition, the adsorption of 1-site CH_4 in all these adsorbents is significantly enhanced by its stronger CH_4-adsorbent potential energy. We note that the adsorption isotherms of CO_2 mixtures with the 1-site and 5-site CH_4 are quite similar in all these carbons, when the pressure is below 0.5 MPa. This indicates that the molecular model of CH_4 does not impose a significant influence on the adsorption of coexisting CO_2 in the low loading region at this temperature. However, the adsorption of CO_2 mixing with the1-site CH_4 is slightly suppressed compared to the 5-site CH_4 at high pressures. As adsorption progresses, the dominant adsorption of CH_4 will further reduce the adsorption volume available for CO_2, and this effect is more significant for the adsorption of CO_2 coexisting with 1-site CH_4. As a consequence, at relatively high pressures, the adsorption of CO_2 mixing

with the 1-site CH_4 is further reduced in all the carbons, but especially in the (10, 10) CNT because of its smaller adsorption volume. The reduction in the amount of CO_2 is also a consequence of the enhanced 1-site CH_4-adsorbent potential energy.

While the adsorption of 1-site CH_4 is enhanced by the stronger adsorbate-adsorbent potential energy, the adsorption of coexisting CO_2 remains almost unaffected at low pressure and decreases slightly at high pressure in these adsorbents. The equilibrium selectivity of the adsorbent for CO_2 relative to CH_4 is calculated as

$$S_{CO_2} = \frac{x_{CO_2} / y_{CO_2}}{x_{CH_4} / y_{CH_4}} \tag{2}$$

where x_i and y_i are the mole fractions of species *i* in the adsorbed phase and the bulk phase, respectively. As illustrated in Figure 7, the selectivity for CO_2 is greatly underestimated by the 1-site CH_4 model in all the adsorbents studied, and it is likely that this observation is somewhat general, and not specific to the adsorbents under study.

It is interesting to note that while the selectivity of (10, 10) CNT increases with bulk pressure, the selectivity in ACF-15 and SiC-DC decreases with pressure. To explore this phenomenon, we first investigated the variation of CO_2-adorbent and CH_4-adsorbent energies versus pressure in (10, 10) CNT, ACF-15 and SiC-DC, illustrated in Figure 8. It is observed that the adsorbate-adsorbent energies in the (10, 10) CNT decrease slightly with increasing pressure. Therefore, the increase of the selectivity of the (10, 10) CNT with pressure could be caused by two factors: either cooperative CO_2-adsorbate interactions or the adsorbate sieving effect. As total loading is increased, the adsorbate-adsorbate energies are enhanced. The increase in the CO_2-adsorbate energy is greater than the CH_4-adsorbate energy as illustrated in Figure 9 and therefore adsorption of CO_2 is promoted over adsorption of CH_4 (Babarao *et al*., 2009). On the other hand, CO_2 has a much smaller effective diameter (0.3033 nm) in its axial direction than the tetrahedral CH_4 (0.381nm for the spherical CH_4 and an approximately similar effective diameter for the tetrahedral CH_4). As adsorption progresses, adsorbates in the nanotube tend to form discrete aggregates, which merge to fill the volume at high pressure. The rotational freedom of CO_2 is almost unconstrained in the (10, 10) CNT, so that CO_2 can adjust its orientation to achieve sterically and energetically favourable configurations that can be accommodated into existing aggregates, as the insertion of CH_4 is rejected. This is analogous to a molecular sieving effect imposed by the pre-adsorbed

molecules. To support this explanation, we conducted simulations in which the CH_4-adorbate energy was calculated at any simulation step where a CO_2 insertion was accepted, with a randomly generated orientation for CH_4 placed at the same position as the centre of mass as the inserted CO_2. We also calculated interaction energies for a CH_4 molecule with a randomly generated orientation placed at the same position as the centre of mass as the inserted CO_2. The insets of Figure 9 (a) and (b) show these specific CO_2-adsorbate and CH_4-adsorbate interaction energies as a function of bulk pressure for the 3-site CO_2 and 5-site CH_4 in the (10, 10) CNT, ACF-15 and SiC-DC. It is clear that this adsorbate sieving effect is greatly enhanced as pressure is increased, as confirmed by the strong repulsive interactions suffered by the virtually inserted CH_4 molecules. As a consequence of both the adsorbate sieving effect and the additional CO_2-adsorbate interactions, the selectivity of the (10, 10) CNT increases with pressure although the adsorbate-adsorbent interactions do not change significantly. The selectivity only increases slightly with pressure as adsorption approaches saturation at high pressure, because the cooperative interactions and the adsorbate sieving effect change less rapidly with pressure, and the increase in the entropic effect due to packing restrictions tends to offset the contributions from these two factors. One can expect that the selectivity of a (10, 10) CNT will actually decrease with increase in pressure at high enough pressures when the adsorbate sieving effect will disappear, and the entropic effect will take over completely, as can be seen in the results of Palmer *et al*.(2011).

From Figure 8, it is clear that the co-adsorption of CO_2/CH_4 in AC-F15 and SiC-DC occurs preferentially in the narrow pores at low pressure, and shifts to larger pores at high pressures. Initially, the selectivities of ACF-15 and SiC-DC are even higher than in the (10, 10) CNT, which can be attributed to the molecular sieving effect. Since both disordered carbons have pores with widths smaller than 0.40 nm, which can only accommodate CO_2 in a linear orientation, the molecular sieving effect is dominant. Since ACF-15 has a larger volume of these narrow pores than SiC-DC, it exhibits a higher selectivity for CO_2 (Farmahini *et al*., 2013; Nguyen *et al*., 2008). It is notable that varying the morphology of these porous carbons does not significantly affect the selectivity of CO_2 relative to CH_4. The insets in Figure 9 show that the adsorbate sieving effect in ACF-15 and SiC-DC is much weaker than in the (10, 10) CNT. Although the adsorption isotherms of CO_2 and CH_4 in the (10, 10) CNT are lower than in the ACF-15 and SiC-DC above 1.0 MPa, the number densities of CO_2 and CH_4 in the (10, 10) CNT are actually much higher than that in the other two porous carbons, due to the high carbon atom density and high degree of confinement in the CNT. Consequently, the

adsorbate sieving effect is much weaker in disordered carbons, compared to the (10, 10) CNT. Accordingly, as illustrated in Figure 8 the rapid reduction in the adsorbate-adsorbent interactions offsets the contribution from the cooperative CO_2-adsorbates interactions and adsorbate sieving effect completely, and leads to the decrease in selectivity with pressure.

3.3 Effect of composition on the adsorption of CO_2/CH_4

As shown above (Figures 3 and 6(b)), the adsorption isotherms of pure CH_4 and CO_2/CH_4 mixture in SiC-DC and ACF-15 are quite similar, so SiC-DC will be chosen to represent the disordered carbons in further discussions. Boutin *et al.* (1994) and Lachet *et al.* (1996) reported that unlike the 5-site model, the 1-site model failed to reproduce the experimental isotherms of CH_4 in $AlPO_4$-5. In addition, we have shown the 1-site CH_4 overestimated the adsorption of CH_4 and underestimated the selectivity for CO_2 in CNTs, ACF-15 and SiC-DC, and further discussion will therefore be based on the 5-site CH_4 and 3-site CO_2. The composition of natural gas found in different reservoirs varies significantly, such that the ratio of CO_2/CH_4 in natural gas has a wide range of distribution (Rojey *et al*., 1997). We investigated three compositions, having CO_2 contents of 5%, 25%, and 50% to reveal the effect of composition on the adsorptive and selective properties of the CNT and SiC-DC.

Figures 10 (a) and (b) respectively depict the isotherms of CO_2 and CH_4 in (10, 10) CNT and in Si-CDC at 300 K for different compositions. The adsorption of CO_2 is completely dominant for adsorption from equimolar mixtures due to the energetic and adsorbate sieving effects. When the concentration of CH_4 is increased to 75%, it is found that the adsorbed amounts of CH_4 in the (10, 10) CNT and in SiC-DC have increased, but are still far below that of CO_2. However, on further increase to 95% CH_4, the adsorption of CH_4 becomes dominant. At a fixed bulk pressure, increasing the concentration of CH_4 in the bulk phase reduces the total adsorbed amount of CO_2 and CH_4. Because CH_4 has a less energetically and sterically favourable molecular configuration for adsorption, the increase in the amount of CH_4 adsorbed fails to compensate for the reduction in the amount of CO_2 in the adsorbed phase.

Varying the composition of the gas mixture affects the tendency of the adsorbate to form clusters, and will therefore change the selectivity. Figure 10 (c) shows how the selectivity of the (10, 10) CNT increases dramatically with increasing concentration of CO_2 in the gas phase. At equimolar bulk concentration, more CO_2 is adsorbed and most of the adsorption space is occupied by aggregates of the linear CO_2 molecules, as is evident from snapshots

presented in Figure 11. This adsorbate structure will preferentially adsorb additional CO_2 molecules and will tend to reject the tetrahedral CH_4 molecules. It is noted that, at a fixed bulk pressure, increasing the concentration of CO_2 in bulk phase increases the adsorbate loading as well as the fraction of CO_2 in adsorbed phase, which subsequently enhances the adsorbate-adsorbate lateral interactions. The combination of increased concentration of CO_2 in the gas phase and the adsorbate sieving effect increases the selectivity in favour of CO_2. In addition, the selectivity increases even more rapidly with increase in pressure for the cases having higher concentration of CO_2 in bulk phase. However, at high pressure, the selectivity of CNT increases only slightly for all the compositions, as the co-adsorption approaches saturation. Moreover, for the equimolar bulk mixture, the selectivity of the (10, 10) CNT tends to decrease above a pressure of 2.5 MPa, which is because of the onset of entropic effects.

As noted earlier, for the gas mixture containing 5% CO_2, the selectivity of SiC-DC decreases with increase in bulk pressure, which is because the adsorbate sieving effect and the cooperative CO_2-adsorbate interactions are too weak to overcome the reduction in the adsorbate-adsorbent interactions. However, as the concentration of CO_2 increases to 25%, it is observed that the selectivity starts to increase slightly above a pressure of 1.5 MPa, which is caused by the enhanced CO_2-adsorbate interactions and the adsorbate sieving effect. Accordingly, for the equimolar bulk mixture, the selectivity starts to increase at lower pressure (0.4 MPa), and increases more rapidly compared to the case of low CO_2 concentrations in bulk phase. We note that changing the composition of gas mixture has less significant influence on the selectivity of SiC-DC for CO_2 compared to the (10, 10) CNT. This is because the confinement in SiC-DC is much weaker than in the CNT (lower intrinsic selectivity for CO_2, excluding the molecular sieve effect). Consequently, as the CO_2 concentration in the bulk phase increases, the increase in the total loading and the fraction of CO_2 in the adsorbed phase is less significant than that in the CNT; this subsequently leads to weaker enhancement in the cooperative CO_2-adsorbates interactions and the adsorbate sieving effect. However, the lower adsorbate density in SiC-DC is also responsible for the weak influence of composition on the selectivity in SiC-DC.

At low bulk pressure, the adsorbed amount of a component is determined by its partial pressure and Henry constant (Nicholson and Parsonage, 1982), and the selectivity for CO_2 follows $S_{CO_2} = K_{CH_4} / K_{CO_2}$. The Henry constant for a specific component is only dependent

on the adsorbate-adsorbent interactions (Nicholson and Parsonage, 1982), and therefore, as observed in Figure 10 (c) and (d), the selectivities of the CNT and SiC-DC for different compositions converge to their corresponding constants, which are independent of the composition of gas mixture. In particular, the selectivity of Si-CDC decreases with increase in the concentration of CO_2 when the bulk pressure is below 0.4 MPa, as shown in Figure 10 (d). Note that, the high selectivity of Si-CDC at low pressures is attributed to a molecular sieving effect, but since the total volume of these narrow pores is very limited, the amount of CO_2 adsorbed into the narrow pores does not increase proportionally when the concentration of CO_2 is increased from 5% to 50%. As a consequence, the selectivity of Si-CDC decreases with CO_2 concentration at low pressures.

3.4 Effects of temperature and diameter on the adsorption of CO_2/CH_4 mixture in CNTs.

We investigated the adsorption of CO_2/CH_4 in the (10, 10) CNT at 300 K, 325 K and 350 K, at a bulk phase mole fraction of CO_2 of 5%. As depicted in Figure 12 (a), the adsorbed amounts of CO_2 and CH_4 both decrease with increase in temperature due to the exothermic nature of adsorption. However, the selectivity of the (10, 10) CNT decreases with increase in temperature as well, indicating the most effective separation of CO_2 from natural gas using CNTs would be conducted at near-ambient temperatures. Similar effects of temperature on the adsorption and separation of CO_2/CH_4 mixtures in ACF-15 and SiC-DC, not shown here, were observed in our simulations.

We also investigated the selectivity in a variety of armchair CNTs with diameters ranging from 0.81 nm to 2.03 nm at 300 K, in order to determine the optimum diameter for separating CO_2 from natural gas. As the diameter was increased from 1.36 nm to 2.03 nm, the selectivity of CNT decreased, as seen in Figure 13. In contrast to the (10, 10) CNT, the contribution of the adsorbate-adsorbent energy to the total energy decreases significantly with adsorbate loading in the (12, 12) and (15, 15) CNTs, since these CNTs are wide enough to accommodate multilayers (Liu and Bhatia, 2013). So, in the (12, 12) and (15, 15) CNTs, the selectivity increases only slightly with bulk pressure, as the reduced confinement partly offsets the contribution from the CO_2-adsorbate pair interactions and the adsorbate sieving effect to enhance the selectivity for CO_2. However, the selectivity does not increase monotonically as diameter is reduced: in the (6, 6) CNT, selectivity is found to increase at pressures close to zero because of the high degree of confinement. At this diameter, the rotational freedom of CO_2 is highly restricted, which dramatically reduces the selectivity with

increase in total loading (Nicholson and Gubbins, 1996). In the larger (7, 7) CNT, the restriction on the orientational configurations of CO_2 is less significant, and therefore the selectivity is higher than in the (6, 6) CNT, even though the confinement is less. However, the selectivity of the (7, 7) CNT increases more rapidly with pressure than that of the (10, 10) CNT, but less rapidly than in the (8, 8) CNT. In comparison to the (10, 10) CNT, the intrinsic selectivity of the (7, 7) CNT is much higher, so that the mole fraction of CO_2 in the adsorbed phase in the (7, 7) CNT is much higher than that in the (10, 10) CNT. Consequently, the adsorbate sieving effect and the CO_2-adsorbates interactions are enhanced in the (7, 7) CNT with increasing the pressure. On the other hand, the restriction on the rotational freedom of CO_2 in the (7, 7) CNT is still strong, as confirmed by the total density distribution of adsorbates in the (7, 7) CNT at 1.0 MPa, depicted in Figure 14. It is seen that while the adsorbates accommodate themselves into a single layer in the (8, 8) CNT at 1.0 MPa, there is insufficient space to form a complete adsorbate layer in the (7, 7) CNT. The interplay between the entropic effect and the adsorbate-adsorbent energy means that the selectivity of the (7, 7) CNT increases less rapidly than in the (8, 8) CNT, but more rapidly than in the (10, 10) CNT.

The separation of CO_2 from natural gas is generally conducted at ambient temperature and atmospheric pressure, with the concentration of CH_4 being around 95% (Martín-Calvo *et al*., 2008). In Figure 15 (a), we have plotted the selectivity and the adsorbed amount of CO_2 as a function of the diameter of the CNT, at a pressure of 0.1MPa and a temperature of 300 K; the selectivity of CNT increases as the diameter increases from 0.81 nm to 0.95 nm, and then decreases with further increase in diameter. The selectivity achieves a maximum value of 8.31 in the (7, 7) CNT with a diameter of 0.95 nm, which also corresponds to the maximum in the amount of CO_2 adsorbed (Figure 15 (b)). Both the selective and the adsorptive properties of the (7, 7) CNT are superior to the disordered carbons. Thus, based on our results, the (7, 7) CNT having diameter of 0.95 nm has the greatest potential for separating CO_2 from natural gas.

4. Conclusions

We have presented a detailed study of the adsorption of CH_4 and CO_2/CH_4 mixture in CNTs and realistic porous carbons, ACF-15 and SiC-DC. It is found that the united atom model of CH_4 always over predicts the adsorption of CH_4 in CNTs and disordered porous carbons compared to the all-atom model, which is attributed to its enhanced potential energy with

pore walls in the united atom model. Further, for the adsorption of CO_2/CH_4 mixtures, while the adsorption of 1-site CH_4 is enhanced in all the carbons, the adsorption of co-existing CO_2 is slightly reduced at high pressure because of loss of adsorption space that is occupied by the additionally adsorbed 1-site CH_4. Consequently, the selectivities of CNTs and disordered carbons for CO_2 relative to CH_4 are severely underestimated compared to the co-adsorption of CO_2 and 5-site CH_4. However, the similarity between the adsorption isotherms of pure CH_4 and CO_2/CH_4 mixtures in ACF-15 and in the much more disordered SiC-DC demonstrates that the morphology of porous carbons has little impact on the adsorptive and selective properties of porous carbons when the pore size distributions as well as the carbon framework densities are similar.

In a (10, 10) CNT the selectivity for CO_2 is an increasing function of pressure, while the selectivity of amorphous AC-F15 and SiC-DC decreases with increase in pressure. This phenomenon is a result of the competition between the adsorbate-adsorbent interaction and the adsorbate-adsorbate interplays. It is also found that increasing the concentration of CO_2 in the gas phase increases the selectivity of the (10, 10) CNT but has an insignificant influence on selectivity in amorphous porous carbons. The adsorbate density in and selectivity of the (10, 10) CNT are much higher than in the other two porous carbons, due to its high carbon density and uniform confined space having high pore wall curvature. Additionally, the adsorbate-adsorbate pair configurations create an adsorbate sieving effect which is dramatically enhanced for the linear CO_2 as the concentration of CO_2 in gas phase is increased. Consequently, the selectivity of the (10, 10) CNT is almost doubled at high pressures when the concentration of CO_2 is increased from 5% to 50%.

Increasing the temperature reduces the selectivity of these carbons. We find that the (7, 7) CNT having a diameter of 0.95 nm adsorbs the maximum amount of CO_2 and has the highest selectivity for CO_2, at 0.1 MPa.

Acknowledgement

One of us (SKB) acknowledges an Australian Professorial Fellowship from the Australian Researches Council. Lang Liu gratefully acknowledges the Chinese Government for a CSC (China Scholarship Council) scholarship. This research has been supported by the Australian Research Council through a grant under the Discovery scheme.

Reference

Allen, M.P., Tildesley, D.J., 1989. Computer simulation of liquids. Oxford University Press, Oxford.

Babarao, R., Hu, Z., Jiang, J., Chempath, S., Sandler, S.I., 2006. Storage and separation of CO_2 and CH_4 in silicalite, C168 schwarzite, and IRMOF-1: a comparative study from Monte Carlo simulation. Langmuir. 23, 659-666.

Babarao, R., Jiang, J., 2009. Unprecedentedly high selective adsorption of gas mixtures in rho zeolite-like metal−organic framework: a molecular simulation study. J. Am. Chem. Soc. 131, 11417-11425.

Babarao, R., Jiang, J., Sandler, S.I., 2009. Molecular simulations for adsorptive separation of CO_2/CH_4 mixture in metal-exposed, catenated, and charged metal−organic frameworks. Langmuir. 25, 5239-5247.

Bhatia, S.K., Nicholson, D., 2012. Adsorption and diffusion of methane in silica nanopores: a comparison of single-site and five-site models. J. Phys. Chem. C. 116, 2344-2355.

Bhatia, S.K., Tran, K., Nguyen, T.X., Nicholson, D., 2004. High-pressure adsorption capacity and structure of CO_2 in carbon slit pores: theory and simulation. Langmuir. 20, 9612-9620.

Boutin, A., Pellenq, R.J.-M., Nicholson, D., 1994. Molecular simulation of the stepped adsorption isotherm of methane in $AlPO_4$-5. Chem. Phys. Lett. 219, 484-490.

Cracknell, R.F., Nicholson, D., Quirke, N., 1993. A grand canonical Monte-Carlo study of Lennard-Jones mixtures in slit shaped pores. Mol. Phys. 80, 885-897.

Cracknell, R.F., Nicholson, D., Quirke, N., 1994. A grand canonical Monte Carlo study of Lennard-Jones mixtures in slit pores; 2: mixtures of two centre ethane with methane. Mol. Simulat. 13, 161-175.

Cracknell, R. F., Nicholson, D., Tennison, S. R., Bromhead, J., 1996 Adsorption selectivity of carbon dioxide with methane and nitrogen in slit shaped carbonaceous micropores: simulation and experiment. Adsorption 2, 193-203.

Dash, R., Chmiola, J., Yushin, G., Gogotsi, Y., Laudisio, G., Singer, J., Fischer, J., Kucheyev, S., 2006. Titanium carbide derived nanoporous carbon for energy-related applications. Carbon. 44, 2489-2497.

Do, D.D., Do, H.D., 2005. Evaluation of 1-site and 5-site models of methane on its adsorption on graphite and in graphitic slit pores. J. Phys. Chem. B. 109, 19288-19295.

Ducrot-Boisgontier, C., Parmentier, J., Faour, A., Patarin, J., Pirngruber, G.D., 2010. FAU-type zeolite nanocasted carbon replicas for CO_2 adsorption and hydrogen purification. Energ Fuels. 24, 3595-3602.

Farmahini, A.H., Opletal, G., Bhatia, S.K., 2013. Structural modelling of silicon carbide-derived nanoporous carbon by hybrid reverse Monte Carlo simulation. J. Phys. Chem. C. 117, 14081-14094.

Gelb, L.D., Gubbins, K.E., 1999. Pore size distributions in porous glasses: a computer simulation study. Langmuir. 15, 305-308.

Gogotsi, Y., Nikitin, A., Ye, H., Zhou, W., Fischer, J.E., Yi, B., Foley, H.C., Barsoum, M.W., 2003. Nanoporous carbide-derived carbon with tunable pore size. Natural Materials. 2, 591-594.

Harris, J.G., Yung, K.H., 1995. Carbon dioxide's liquid-vapor coexistence curve and critical properties as predicted by a simple molecular model. J. Phys. Chem. 99, 12021-12024.

Herm, Z.R., Swisher, J.A., Smit, B., Krishna, R., Long, J.R., 2011. Metal−organic frameworks as adsorbents for hydrogen purification and precombustion carbon dioxide capture. J. Am. Chem. Soc. 133, 5664-5667.

Heuchel, M., Davies, G.M., Buss, E., Seaton, N.A., 1999. Adsorption of carbon dioxide and methane and their mixtures on an activated carbon: simulation and experiment. Langmuir. 15, 8695-8705.

Hirschfelder, J.O., Curtiss, C.F., Bird, R.B., 1954. Molecular theory of gases and liquids. John Wiley, New York.

Kunz, O., Wagner, W., 2012. The GERG-2008 wide-range equation of state for natural gases and other mixtures: an expansion of GERG -2004. J. Chem. Eng. Data. 57, 3032-3091.

Kurniawan, Y., Bhatia, S.K., Rudolph, V., 2006. Simulation of binary mixture adsorption of methane and CO_2 at supercritical conditions in carbons. AIChE J. 52, 957-967.

Lachet, V., Boutin, A., Pellenq, R.J.-M., Nicholson, D., Fuchs, A.H., 1996. Molecular simulation study of the structural rearrangement of methane adsorbed in aluminophosphate $AlPO_4$-5. J. Phys. Chem. 100, 9006-9013.

Liu, B., Smit, B., 2009. Comparative molecular simulation study of CO_2/N_2 and CH_4/N_2 separation in zeolites and metal−organic frameworks. Langmuir. 25, 5918-5926.

Liu, B., Smit, B., 2010. Molecular simulation studies of separation of CO_2/N_2, CO_2/CH_4, and CH_4/N_2 by ZIFs. J. Phys. Chem. C. 114, 8515-8522.

Liu, L., Bhatia, S.K., 2013. Molecular simulation of CO_2 adsorption in the presence of water in single-walled carbon nanotubes. J. Phys. Chem. C. 117, 13479-13491.

Lu, C., Bai, H., Wu, B., Su, F., Hwang, J.F., 2008. Comparative study of CO_2 capture by carbon nanotubes, activated carbons, and zeolites. Energ Fuels. 22, 3050-3056.

Martín-Calvo, A., García-Pérez, E., Manuel Castillo, J., Calero, S., 2008. Molecular simulations for adsorption and separation of natural gas in IRMOF-1 and Cu-BTC metal-organic frameworks. Phys. Chem. Chem. Phys. 10, 7085-7091.

Nguyen, T.X., Bae, J.-S., Bhatia, S.K., 2009. Characterization and adsorption modeling of silicon carbide-derived carbons. Langmuir. 25, 2121-2132.

Nguyen, T.X., Cohaut, N., Bae, J.-S., Bhatia, S.K., 2008. New method for atomistic modeling of the microstructure of activated carbons using hybrid reverse Monte Carlo simulation. Langmuir. 24, 7912-7922.

Nicholson, D., Gubbins, K.E., 1996. Separation of carbon dioxide–methane mixtures by adsorption: effects of geometry and energetics on selectivity. J. Chem. Phys. 104, 8126-8134.

Nicholson, D., Parsonage, N.G., 1982. Computer simulation and the statistical mechanics of adsorption. Academic Press, New York.

Palmer, J.C., Moore, J.D., Roussel, T.J., Brennan, J.K., Gubbins, K.E., 2011. Adsorptive behavior of CO_2, CH_4 and their mixtures in carbon nanospace: a molecular simulation study. Phys. Chem. Chem. Phys. 13, 3985-3996.

Pevida, C., Plaza, M.G., Arias, B., Fermoso, J., Rubiera, F., Pis, J.J., 2008. Surface modification of activated carbons for CO_2 capture. Appl. Surf. Sci. 254, 7165-7172.

Presser, V., Heon, M., Gogotsi, Y., 2011. Carbide-derived carbons – from porous networks to nanotubes and graphene. Adv. Funct. Mater. 21, 810-833.

Przepiórski, J., Skrodzewicz, M., Morawski, A.W., 2004. High temperature ammonia treatment of activated carbon for enhancement of CO_2 adsorption. Appl. Surf. Sci. 225, 235-242.

Rojey, A., Jaffret, C., Cornot-Gandolphe, S., Durand, B., Jullian, S., Valaris, M., 1997. Natural gas: production, process, transport. Editions Technip, Paris.

Skoulidas, A.I., Ackerman, D.M., Johnson, J.K., Sholl, D.S., 2002. Rapid transport of gases in carbon nanotubes. Phys. Rev. Lett. 89, 185901.

Skoulidas, A.I., Sholl, D.S., Johnson, J.K., 2006. Adsorption and diffusion of carbon dioxide and nitrogen through single-walled carbon nanotube membranes. J. Chem. Phys. 124, 054708.

Steele, W.A., 1978. The interaction of rare gas atoms with graphitized carbon black. J. Phys. Chem. 82, 817-821.

Sun, Y., Spellmeyer, D., Pearlman, D.A., Kollman, P., 1992. Simulation of the solvation free energies for methane, ethane, and propane and corresponding amino acid dipeptides: a critical test of the "bond-pmf" correction, a new set of hydrocarbon parameters, and the gas phase-water hydrophobicity scale. J. Am. Chem. Soc. 114, 6798-6801.

Tang, Y.W., Chan, K.Y., 2004. The dot and line method: a long range correction to coulomb interaction in a cylindrical pore. Mol. Simulat. 30, 63-70.

Zhang, Q., Chan, K.Y., Quirke, N., 2009. Molecular dynamics simulation of water confined in a nanopore of amorphous silica. Mol. Simulat. 35, 1215-1223.

List of Tables

Table 1. Lennard–Jones parameters, partial charges and configurational parameters for the EPM2 CO_2, 1-site and 5-site CH_4

Molecule	$\varepsilon / k_B (K)$	σ (nm)	q (e)	l (nm)	θ (deg)
Carbon dioxide					
C—C	28.129	0.2757	+0.6512		
O—O	80.507	0.3033	-0.3256		
C—O	47.588	0.2895		0.1149	
O—C—O					180.0
Methane 1-site					
CH_4	148.1	0.381			
Methane 5-site					
C—C	55.055	0.34	-0.66		
H—H	7.901	0.265	+0.165		
C—H	20.856	0.3025		0.109	
H—C—H					109.5

List of Figures

Figure 12. (a) Adsorption isotherms of CO_2 and CH_4 in (10, 10) CNT, and (b) pressure variation of the CO_2 selectivity of (10, 10) CNT, at 300 K, 325 K and 350 K. The mole fraction of CO_2 is 5% in gas phase.

Figure 13. Pressure variation of the CO_2 selectivity of CNTs of different diameter at 300 K, for 5% CO_2 in gas phase.

Figure 14. Total adsorbate density distribution in CNTs, at 1.0 MPa bulk pressure.

Figure 15. Variation of (a) CO_2 selectivity of CNT, and (b) adsorbed amount of CO_2, with CNT diameter, at 0.1 MPa and 300 K, for CO_2/CH_4 bulk mixture having 5% CO_2.

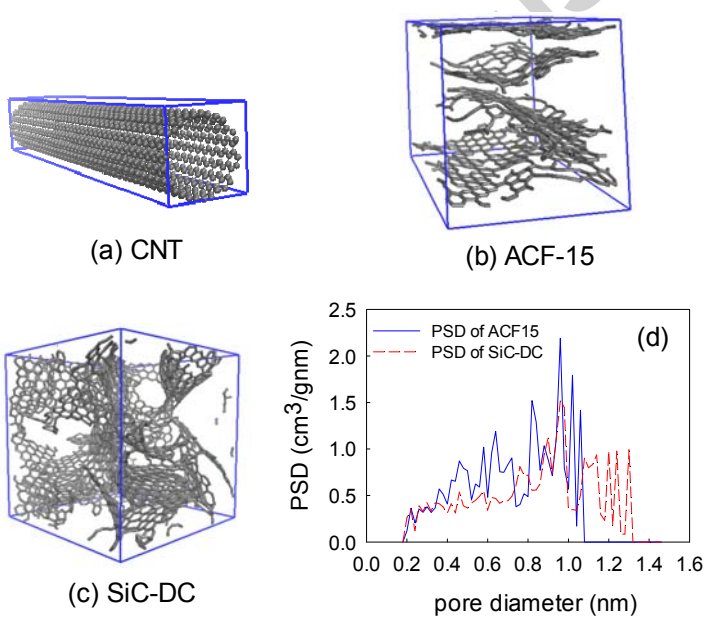

Figure 1. Atomistic configurations of (a) CNT, (b) ACF-15, and (c) SiC-DC, and (d) the geometric pore size distributions of ACF-15 and SiC-DC.

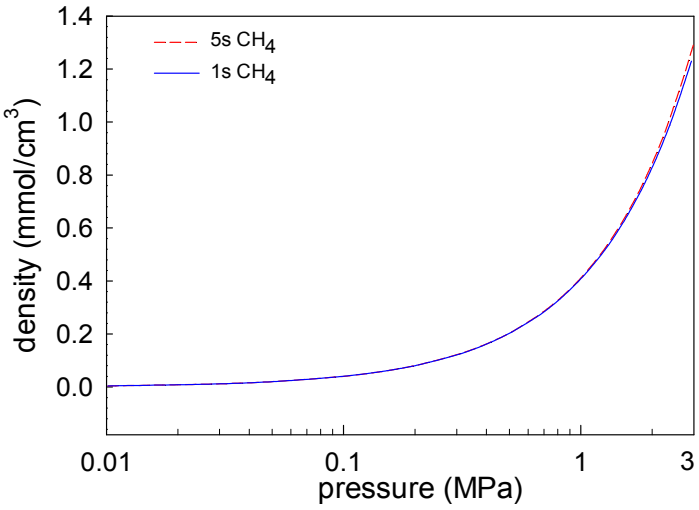

Figure 2. Bulk isotherms of 5-site and 1-site CH_4, at 300 K.

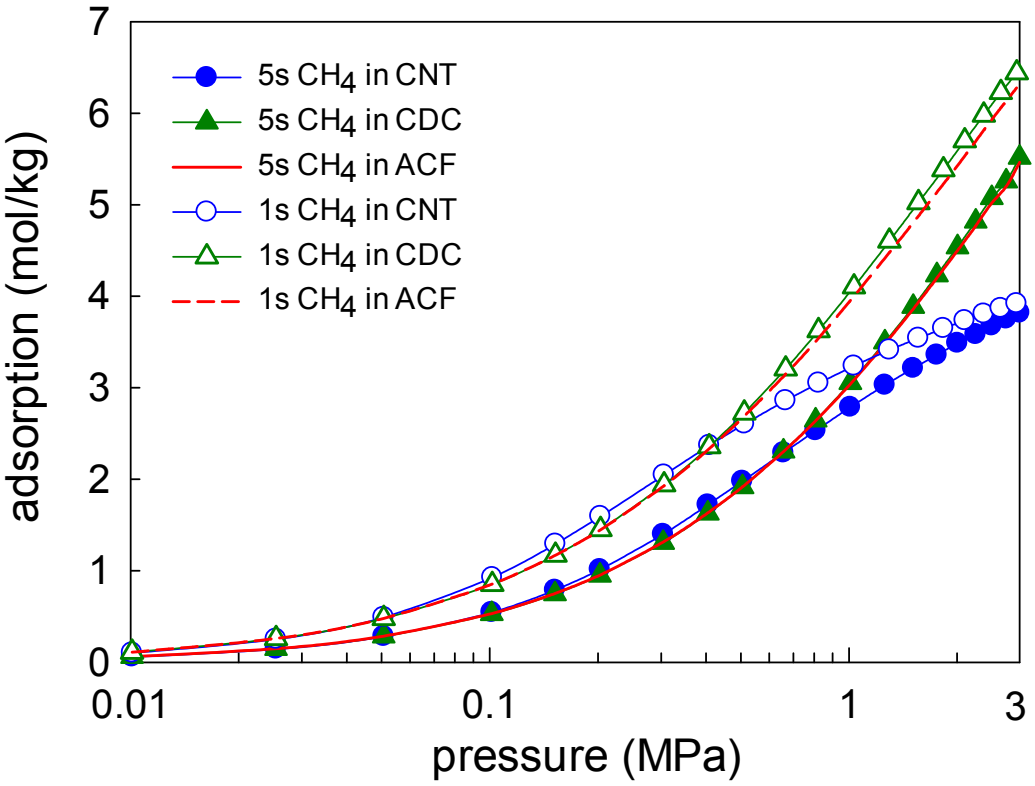

Figure 3. Adsorption isotherms of 1-site and 5-site CH_4 in (10, 10) CNT, ACF-15, and SiC-DC at 300 K.

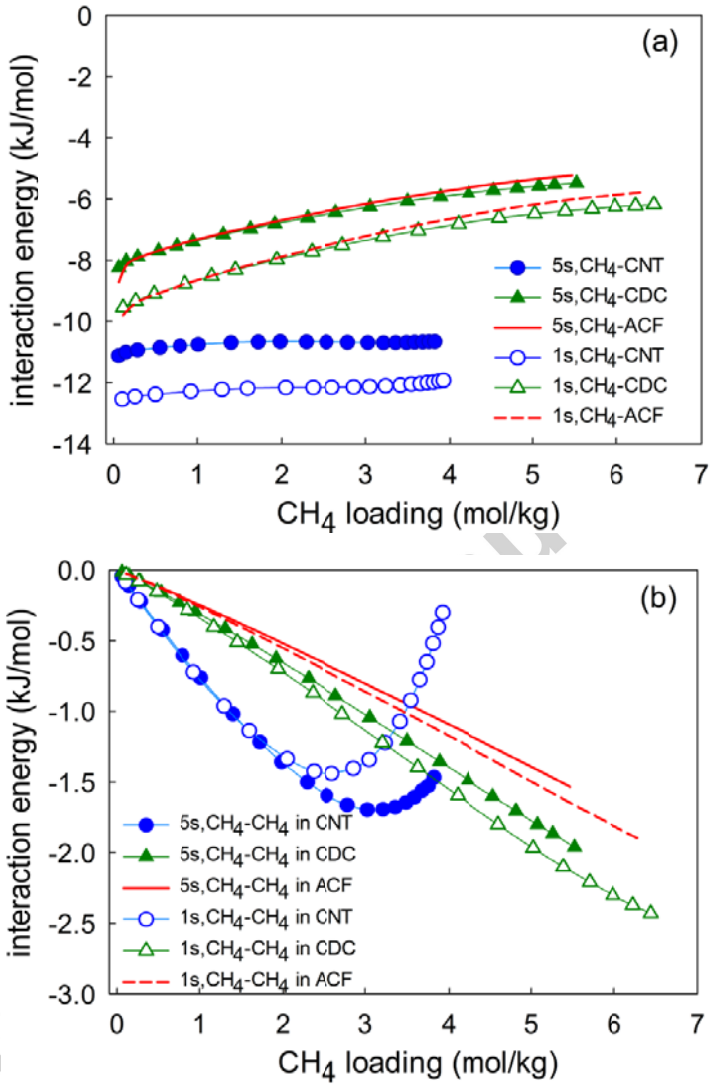

Figure 4. Loading variation of (a) CH_4-adsorbent, and (b) CH_4-CH_4 interaction energies, in (10, 10) CNT, SiC-DC and ACF-15 at 300 K, from GCMC simulations.

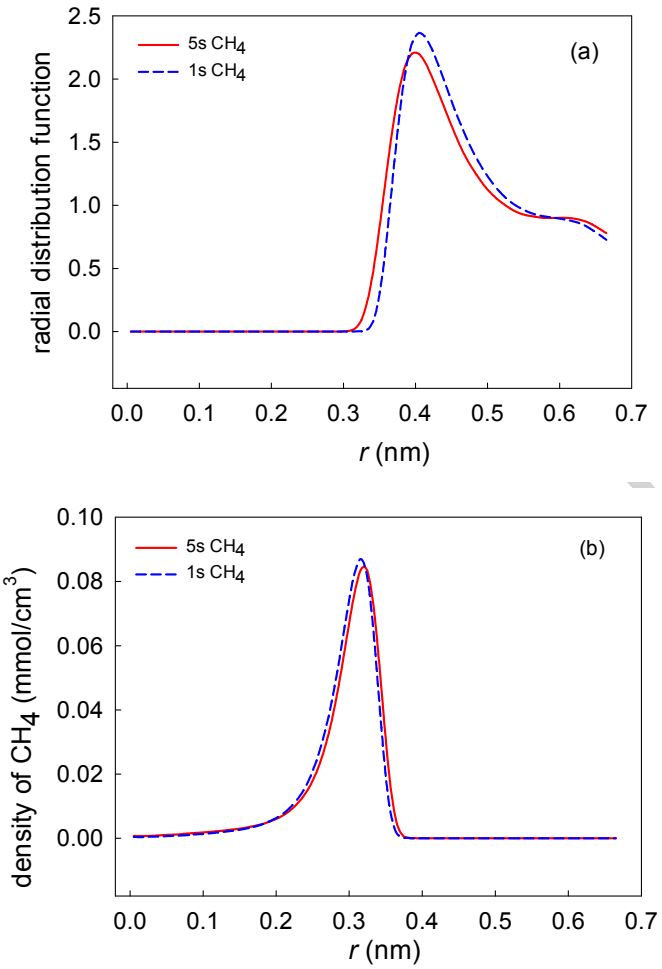

Figure 5. (a) Radial distribution functions, and (b) density distributions of the1-site and 5-site CH_4 in (10, 10) CNT.

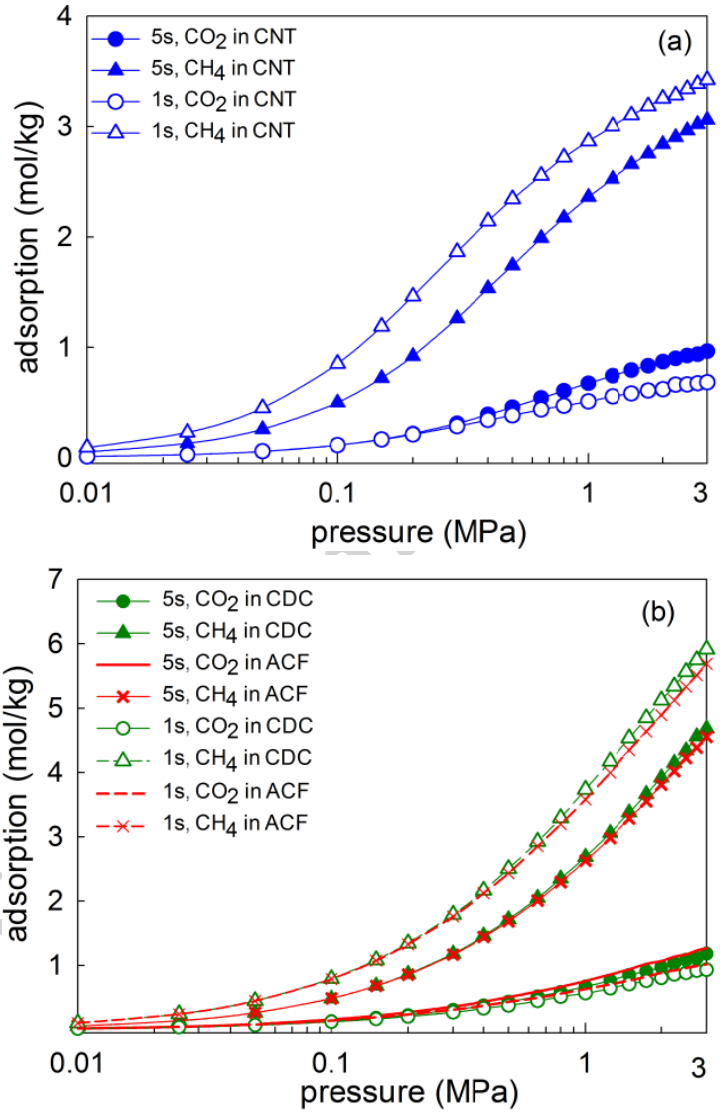

Figure 6. Adsorption isotherms of CO_2 and CH_4 in (a) (10, 10) CNT, (b) SiC-DC and ACF-15 at 300 K. The molar content of CO_2 in the CO_2/CH_4 bulk mixture phase is 5%.

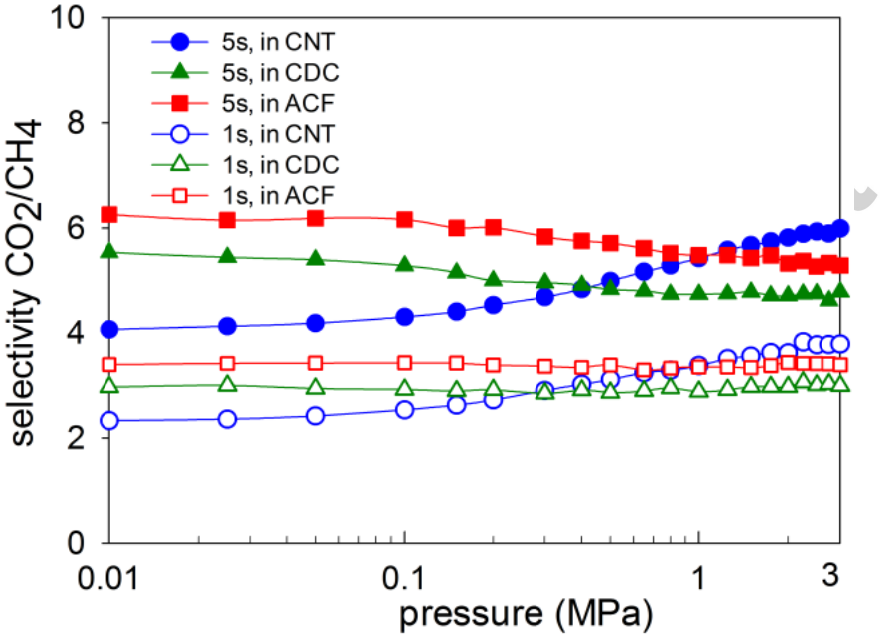

Figure 7. Pressure variation of CO_2 selectivities of (10, 10) CNT, SiC-DC and ACF-15, for 1-site and 5-site CH_4 at 300 K. The bulk phase CO_2/CH_4 mixture has 5% CO_2.

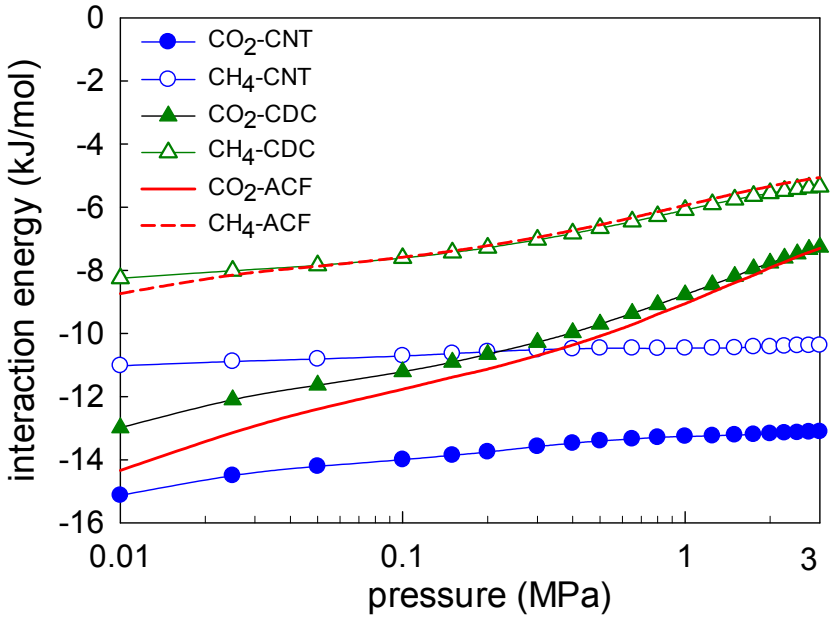

Figure 8. Variation of CO_2-adsorbent and 5-site CH_4-adsorbent interaction energies with pressure in (10, 10) CNT, SiC-DC and ACF-15 at 300 K. The bulk phase has 5% (mole percent) CO_2.

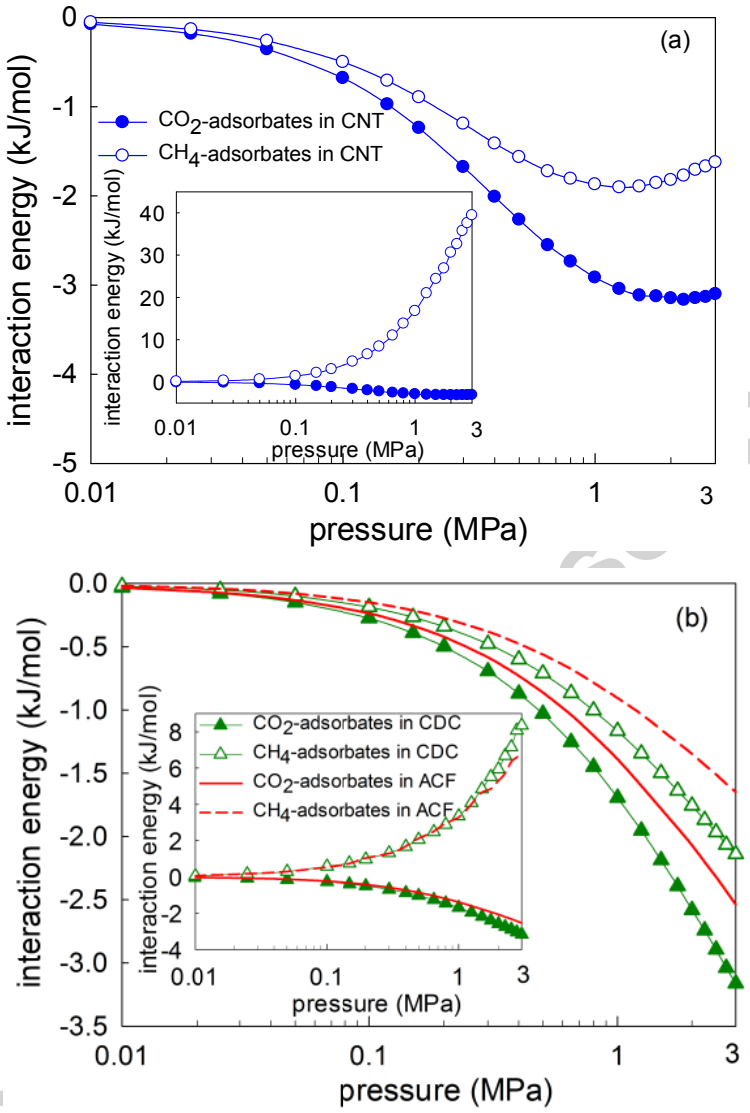

Figure 9. Pressure variation of CO_2-adsorbate and 5-site CH_4-adsorbate interaction energies, in (a) (10, 10) CNT, and (b) SiC-DC, ACF-15, at 300 K. The insets compare CO_2-adsorbate and 5-site CH_4-adsorbate interaction energies using CH_4 to replace the CO_2 at the same adsorption site. The bulk phase has 5% (mole percent) CO_2.

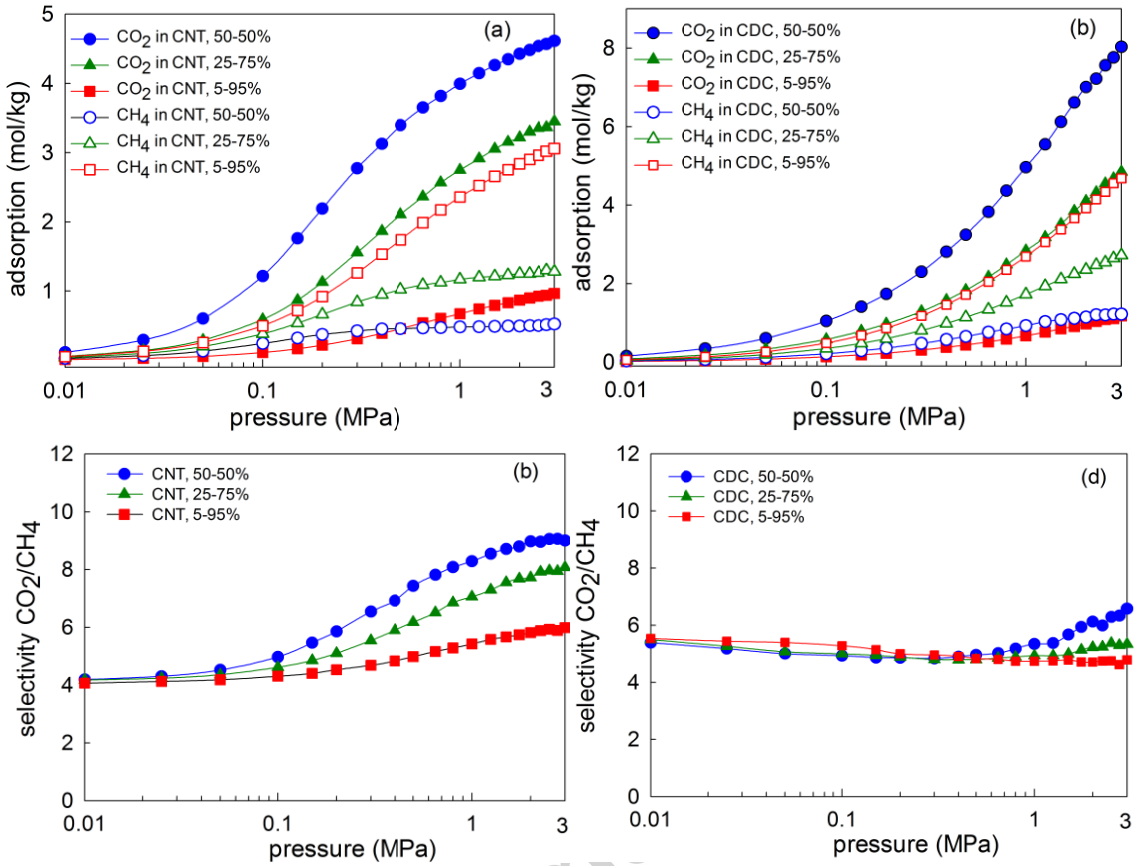

Figure 10. Adsorption isotherms of CO_2 and CH_4 in (a) (10, 10) CNT, (b) SiC-DC, and pressure variation of the selectivities of (c) (10, 10) CNT, and (d) SiC-DC, 300 K. Three CO_2/CH_4 mixture compositions are considered, having CO_2 contents of 5%, 25% and 50%.

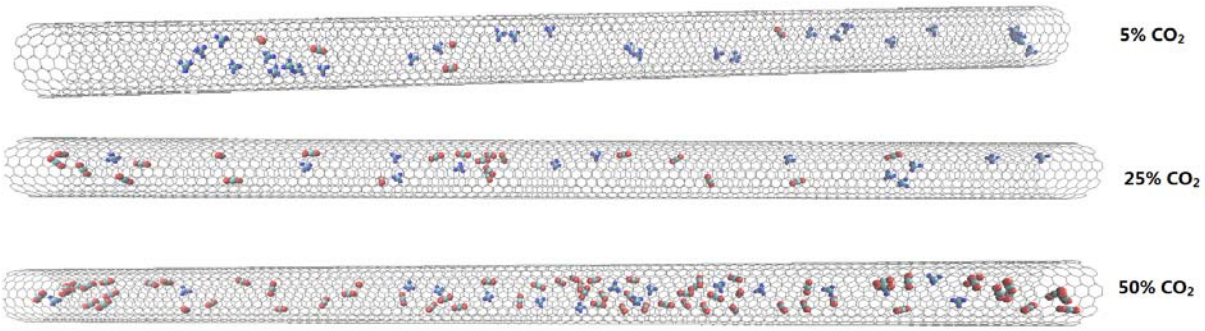

Figure 11. Snapshots of configuration of adsorbed CO_2/CH_4 mixtures of different composition in (10, 10) CNT, at 0.1MPa bulk pressure and 300 K.

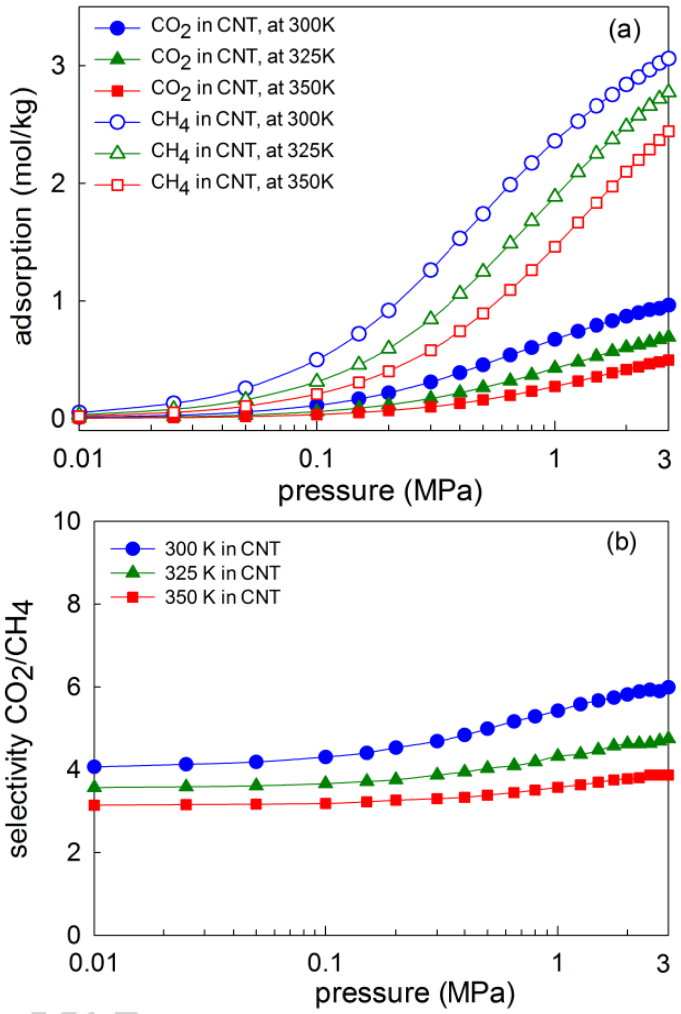

Figure 12. (a) Adsorption isotherms of CO_2 and CH_4 in (10, 10) CNT, and (b) pressure variation of the CO_2 selectivity of (10, 10) CNT, at 300 K, 325 K and 350 K. The mole fraction of CO_2 is 5% in gas phase.

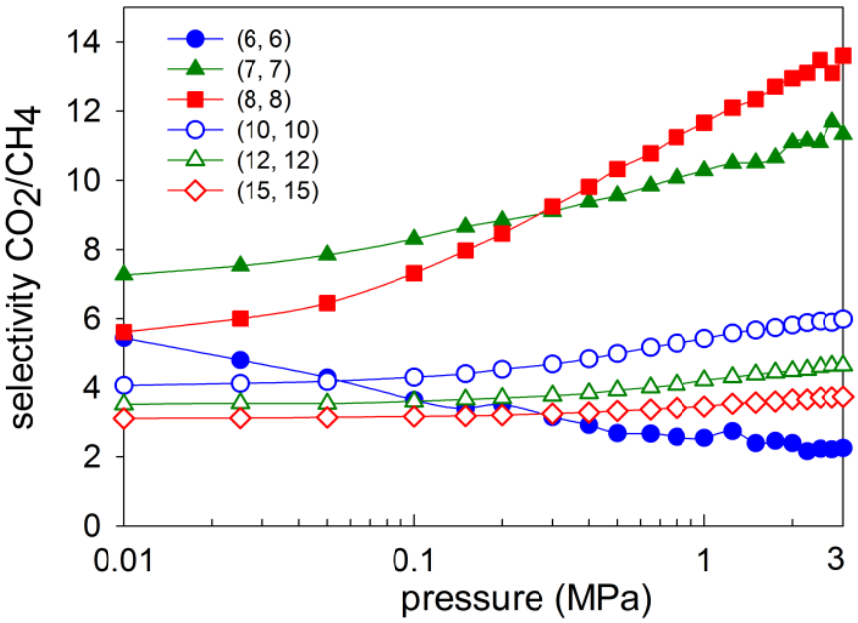

Figure 13. Pressure variation of the CO_2 selectivity of CNTs of different diameter at 300 K, for 5% CO_2 in gas phase.

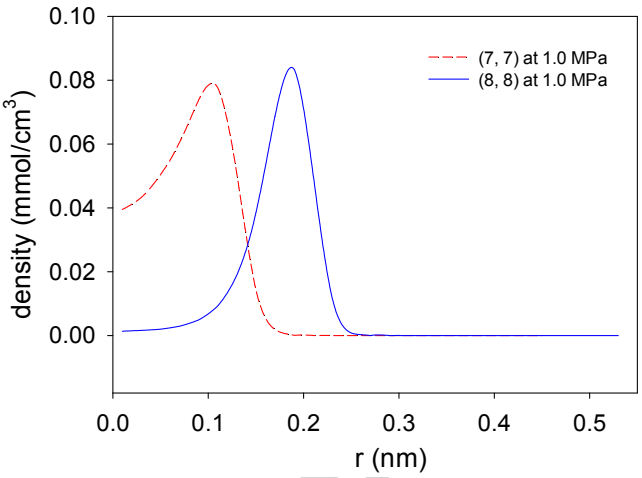

Figure 14. Total adsorbate density distribution in CNTs, at 1.0 MPa bulk pressure.

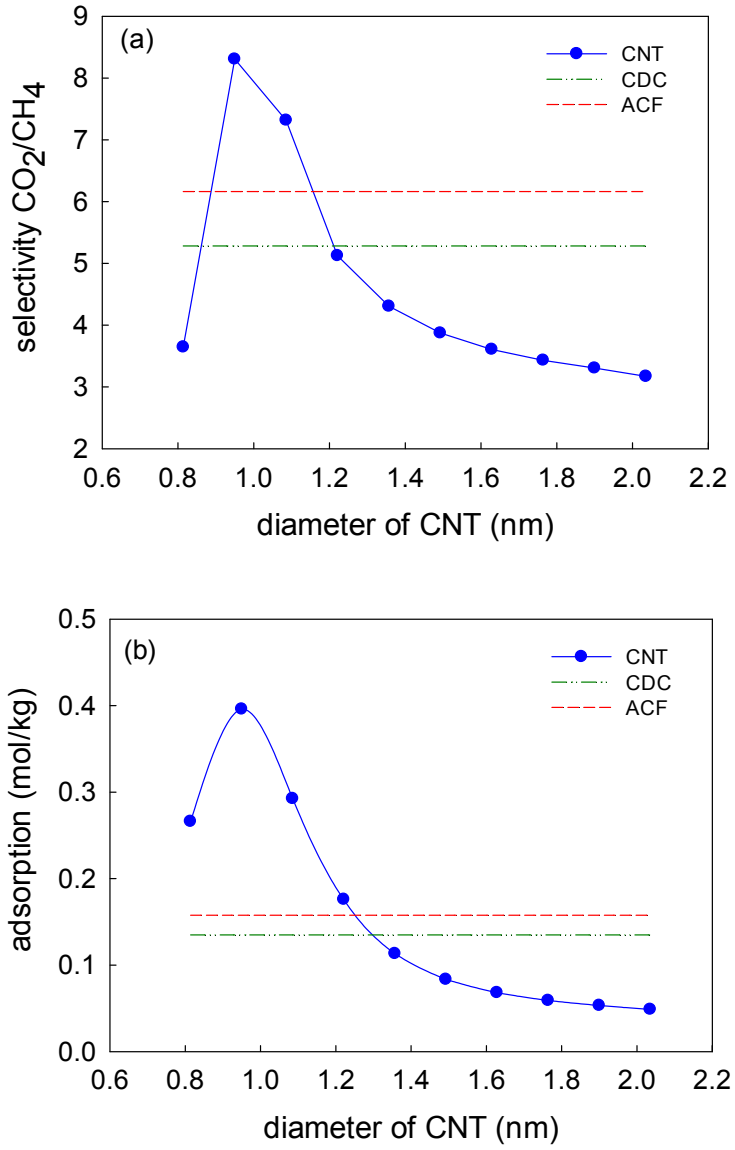

Figure 15. Variation of (a) CO_2 selectivity of CNT, and (b) adsorbed amount of CO_2, with CNT diameter, at 0.1 MPa and 300 K, for CO_2/CH_4 bulk mixture having 5% CO_2.

Research Highlights

- Simulation of adsorption of CH_4 and CH_4/CO_2 mixtures in nanoporous carbons.
- CO_2 selectivities are underestimated using a single site molecular model of CH_4.
- Extent of disorder of porous carbon models has little impact on CO_2 selectivity
- Increased CO_2 fraction improves selectivity in a CNT but not in disordered carbons.
- A (7, 7) carbon nanotube offers best performance for CO_2/CH_4 separation.

Graphical Abstract